Effect of Compositional Variation of Cr_3C_2-NiCr Coating on the Corrosion Behviour at 550°C

Rakesh Bhatia[1*], Hazoor Singh[2] and Buta Singh Sidhu[3]
[1,2]*Yadavindra College of Engineering, Punjabi University,*
G.K. Campus, Talwandi Sabo, Bathinda, Punjab–151302, India
[3]*I.K. Gujral Punjab Technical University,*
Jalandhar, Kapurthala Highway, Kapurtala Punjab, India
*E-mail: *rakesh_lit@yahoo.co.in*

Abstract—*In the current investigation two different compositions of alloy coating powder Cr_3C_2-(Ni-20Cr) were deposited on T-91 boiler tube steel by High Velocity Oxy Fuel (HVOF) spray technique to study the effect of composition variation on corrosion behaviour. The corrosion performance at 550°C of coated as well as uncoated boiler tube steel was evaluated in an aggressive environment of Na_2SO_4–60% V_2O_5 under cyclic conditions. The kinetics of the corrosion was approximated by the weight change measurements, made after each cycle for 50 cycles. X-ray diffraction (XRD), scanning electron microscopy/ energy dispersive X-ray analysis (SEM/EDAX) techniques were used to analyze the corrosion products. The bare steel suffered accelerated corrosion in the form of spalling of the scale. Both the coatings successfully resisted corrosion attack, which may be attributed to the formation of oxides of nickel and chromium. 65%Cr_3C_2-35% (Ni-20Cr) coated sample has shown minimum weight gain and provided highest protection against corrosion as compared to 75%Cr_3C_2-25% (Ni-20Cr) coated and uncoated T-91 sample.*

Keywords: *High Velocity Oxy Fuel (HVOF), Corrosion, Corrosion Resistance, Protective Coatings*

INTRODUCTION

Erosion-Corrosion of boiler tube steel in power plants is a major operating problem as it results in downtime and periodic shutdowns, which in turn accounts for a significant fraction of the total operating cost of power plants. Depletion of high grade fuels, the usage of residual fuel is common in most of the energy generation systems. Residual fuel contains sodium, vanadium and sulphur as impurities [1–3]. Sodium and sulphur forms Na_2SO_4 during combustion, whereas vanadium reacts with oxygen to form vanadium oxide (V_2O_5). These compounds deposit on the surface of the material and induce accelerated oxidation in systems [4]. Otero *et al* concluded that the reaction rate between Na_2SO_4 and V_2O_5 depends both on temperature and the molar ratios [5]. Further it was concluded that a mixture of Na_2SO_4-60% V_2O_5 is the lowest eutectic temperature mixture and is extremely corrosive as it has a low melting point of 550°C [6–7].

The atmosphere in power plant boilers has sufficient free oxygen content to account for a combined erosion–corrosion process, consisting of an oxidizing gas at elevated temperature carrying erosive fly ashes, which impact against metallic surfaces [8]. This form of corrosion consumes the material at very unpredictably rate [9].

Preventing and controlling corrosion depend upon the specific material to be protected, environmental concerns such as soil resistivity, humidity and exposure to saltwater or industrial environments, the type of product to be processed or transported and many other factors [10]. A coating can be used on the surface of an object made of another material, with the aim of obtaining required technical or decorative properties [11].

Continuously rising cost of the materials as well as increased material requirements, the coating techniques have been given much more importance in recent times. Coatings can add value to products up to 10 times the cost of the coating [12]. Among the coating techniques, the thermal spraying has grown into a well accepted industrial technology in which a superior material layer is deposited over a base metal or substrate either to improve the surface characteristic like erosion resistance, wear resistance, corrosion resistance etc. [13]. HVOF thermal spray process is reported to be versatile technology and has been adopted by many industries due to its flexibility, cost effectiveness and the superior quality of coating produced [14–15]. The HVOF coatings have high hardness, low oxidation, high abrasion resistance, low porosity, high density, superior bond strength, thick coating, fine finishing capability and lower oxide content [2, 16–21].

Cr_3C_2-NiCr cermet coatings have been extensively used to mitigate abrasive and erosive wear at high temperatures up to 850°C [22–23]. The corrosion resistance is provided by NiCr matrix while the wear resistance is mainly due to the carbide ceramic phase. Researchers agree that carbide-based coatings provide excellent erosion-corrosion protection, but disagree on the optimum amount of carbide for maximum erosion-corrosion resistance [24–26].

So in the present work the percentage of chromium carbide (Cr_3C_2) and nickel chrome (Ni-20Cr) powders in the coating composition was varied to find out its effect on the corrosion behaviour of coatings at 550°C.

EXPERIMENTAL DETAILS

Substrate Material

The boiler tube steel T-91 with chemical composition as shown in Table 1, have been used as substrate material. The tube material was obtained from Guru Nanak Dev

Thermal Power Plant, Bathinda and samples with dimensions 22 mm × 15 mm × 3 mm were prepared.

Table 1: Chemical Composition (wt.%) of Boiler Tube Steel (T-91)

Nb	Mn	Si	Cr	Mo	Ni	C	Fe
0.07	0.5	0.4	9	0.95	0.4	0.11	Balance

The specimens were polished with SiC papers down to180 grit, and subsequently grit-blasted with alumina powders (Grit 45) before development of the coatings by the HVOF process. Specimens were prepared manually and all care was taken for any structural changes in the specimens.

Formulation of Coating

Commercially available compositions of 65%Cr_3C_2-35% (Ni-20Cr) and 75% Cr_3C_2-25 % (Ni-20Cr) alloy powders were used for formulating coatings. Detail of the coating powder and the designations of coating are given in Table 2. The coatings were developed at M/S Metallizing Equipment Co. Pvt. Ltd. (Jodhpur, India) by using commercial Hipojet-2100 HVOF thermal spray system. Liquefied petroleum gas (LPG) was used as a fuel. All of the process parameters were kept constant throughout the coating process. The specimens were cooled with compressed air jets during and after spraying. The spray parameters used for the Hipojet-2100 system are given in Table 3.

Table 2: Composition, Particle Size and Designation of Coating Powders

Coating Powder	Type	Size
65%Cr3C2-35% (Ni-20Cr)	Agglomerated Sintered	-45 + 15 µm
75%Cr3C2-25% (Ni-20Cr)	Agglomerated Sintered	-45 + 15 µm

Table 3: Spray Parameters as Employed during HVOF Spraying

Oxygen flow rate	250 LPM
Fuel (LPG) flow rate	60 LPM
Airflow rate	900 LPM
Spray distance	20 cm
Fuel pressure	8 kg/cm2
Oxygen pressure	9 kg/cm2
Air pressure	5 kg/cm2
Powder feed rate	28 g/min

LPM* Litres per Minute

Characterization of the Coatings

The coated samples were mirror polished and then subjected to XRD, SEM/EDAX analysis to characterize the surface and cross-sectional morphology of the coatings. The XRD analysis was carried out with a Diffraction patterns obtained by Bruker AXS D-8 Advance Diffractometer (Germany) with CuKα radiation. The specimens were scanned in 2θ range of 10 to 110° and the intensities were recorded at a chart speed of 1 cm/min and with Goniometer speed 10/min. The diffractometer interfaced with software provides 'd' values directly on the diffraction pattern. A scanning electron microscope (JSM-6610, Jeol, New York) with an EDAX attachment (Oxford, UK) was used for SEM/EDAX analysis. The porosity measurements were made with an image analyzer with Dewinter Material Plus 1.01 software based on ASTM B 276. The image was obtained through the attached PMP3 inverted metallurgical microscope with stereographic imaging. To identify the cross-sectional details, the samples were cut across the cross section, mounted in transoptic powder. The specimens were polished manually using emery papers of different grit sizes and grades. Finally, the specimens were mirror polished and washed thoroughly with water, and dried in hot air to remove any moisture.

The microhardness of the coatings was measured by the Microhardness tester (Omnitech, India). A 300 g load was provided to the needle for penetration and hardness value was calculated Surface roughness of the specimens was measured by Surface roughness tester (Mitutoyo Model SJ 201, Japan).

Molten Salt Corrosion Tests

Cyclic studies were performed in molten salt (Na_2SO_4-60 wt. %V_2O_5) for 50 cycles. Each cycle consisted of 1 hr heating at 550°C in a silicon carbide tube furnace followed by 20 min cooling at room temperature; the cyclic conditions have been chosen to create a more aggressive situation of corrosion attack.

The specimens were washed with acetone and heated in an oven to about 250°C. The specimens were heated to ensure proper adhesion of the salt layer. Then a layer of Na_2SO_4-60%V_2O_5 mixture prepared in distilled water was applied uniformly on the warm specimens with the help of a camel hair brush. The amount of the salt coating was kept in the range of 3.0 to 5.0 mg/cm^2. The salt-coated specimens as well as the alumina boats were then kept in the oven for 3 to 4 h at 100 °C and weighed before exposing to corrosion tests in the tube furnace. The salt mixture was applied on the surface only once in the beginning of the test, and it was not replenished during the test. The studies were performed for uncoated as well as coated specimens for the purpose of comparison. During corrosion runs, the weight of boats and specimens were measured together at the end of each cycle, with the help of Electronic Balance Machine Model 06120 (Contech, India) with a sensitivity of 1 mg. The spalled scale was also included at the time of measurements of weight change to determine total rate of corrosion. The surface of the corroded specimens was visually observed to record color, spalling and peeling of scale during cyclic corrosion. Efforts were made to formulate the kinetics of corrosion. XRD, SEM/EDAX techniques were used to analyze the corrosion products.

RESULTS AND DISCUSSIONS

Thickness, Porosity, Surface Roughness and Micro Hardness of the Coatings

The thickness was monitored during the process of depositing the coatings with a Minitest-2000 thin film thickness gauge (Elektro-Physik Koln Company, Germany; precision ±1 μm), to obtain the coatings with uniform thickness. To verify the thickness of the coatings, the back scattered electron (BSE) images indicating three regions namely substrate, coating and epoxy (resin) were taken. Average thickness of the coatings has been measured from these BSEI micrographs and the data have been reported in Table 4. The cross-sectional morphology (Fig. 1) of the coatings shows that the coatings in general exhibit characteristic splat-like, layered morphologies due to the deposition and resolidification of molten or semi molten powder particles. The jet-black dark dots are expected to be the porosity. The images show comparatively denser microstructure along the cross-section. Some superficial pores in the microstructure are present in most of the cases, which are mostly found in the vicinity of the coating/ substrate interface. Porosity in the coating during thermal spraying is an important parameter. Due to this physical property corrosion resistance of different thermal spraying coatings differs. Porosity lead the corrosion accelerators/ species to the substrate and may result in corrosion attack [27].

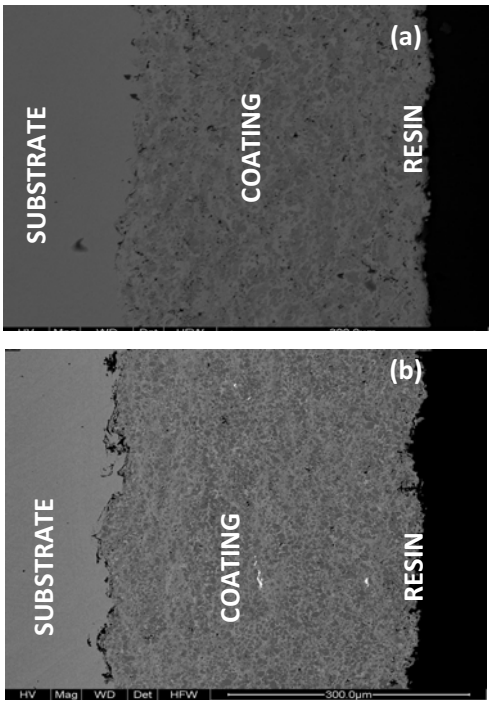

Fig. 1: SEM Cross-Sectional Microstructures of (a) 65%Cr_3C_2-35% (Ni-20Cr) Coating (b) 75%Cr_3C_2-25% (Ni-20Cr) Coating

The porosity, mean of five measurements performed for each coating is shown in Table 4.

The microhardness along the cross section of the coatings as a function of distance from the coating-substrate interface indicated 862 Hv as the maximum average value of the microhardness for 75%Cr_3C_2-25% (Ni-20Cr) coating. This value is much higher than the microhardness of the substrate steel which was found to be 317 Hv only. The average microhardness of the coatings is reported in Table 4.

Corrosion Kinetics

Weight change data is compiled in Fig. 2 in the form of a plot, where the cumulative weight gains per unit surface area (mg/cm^2) is plotted with respect to time expressed in number of cycles. The values of overall weight gain after 50 cycles of hot corrosion for the uncoated and coated T-91 steel at 550°C are also reported in Table 4. Further, the weight gain square (mg^2/cm^4) data is also plotted as a function of time (number of cycles) as shown in Fig. 3 to establish the rate law for the corrosion. It can be immediately inferred from the plot that all the coated steels followed the parabolic rate law of oxidation. Parabolic rate constant (Kp) values as calculated from the linear regression fitted curves are reported in Table 4.

Table 4: Thickness, Porosity, Average Microhardness and XRD Phases of Different as Coated Samples

Coating	Thickness	Porosity (%)	Average Micro Hardness (Hv)	Weight Gain (mg/ cm^2)	Parabolic Constant (Kp) x 10-10 g2 cm-4 s-1
Uncoated T-91	----	------	317	10.6529	12.952
75%Cr_3C_2-25% (Ni-20Cr) coating	350 μm	<1.5%	862	1.2782	0.79
65%Cr_3C_2-35% (Ni-20Cr) coating	350 μm	< 1.5%	688	1.0462	0.1222

Xrd Analysis

The XRD analysis identified iron oxide as the main phase for the corroded uncoated steel along with weak peaks of chromium oxide. For all the coated and subsequently corroded steel the XRD analyzed Cr_2O_3 and $NiCr_2O_4$ as the common phase with weak peaks for the phases of Na and V as shown in Fig. 4.

Surface Analysis of Oxide Scale

Surface of uncoated T-91 steel after cyclic corrosion in Na_2SO_4–60% V_2O_5 environment for 50 cycles at 550°C seems to be consisting of flakes of scale and sharp

whiskers. The EDS analysis reveals the scale rich in Fe and O, which indicates the possibility of formation of Fe_2O_3. Small amount of Cr and marginal amount of Ni are also indicated at the points of analysis, thereby predicting the possibility of formation of Cr_2O_3 and NiO. Formation of Oxides of Fe and Cr has been validated by the XRD analysis. Significant amounts of Mo and Nb are also seen at the points of investigation indicating the diffusion of elements from substrate into the coating.

EDAX analysis of the surface of corroded 65%Cr_3C_2-35% (Ni-20Cr) coating in Fig.5 shows the presence of Ni and Cr along with Na, S, Mo and V. Generation of corrosive species of vandates and sulphates for starting corrosion process due to application of the molten salt applied on the surface can be observed.

The top surface of corroded 75%Cr_3C_2-25% (Ni-20Cr) coating seems to be consisting of corrosive species even after completion of 50 cycles in form of Na, S and V. Sufficient amount of O was also observed on the top surface. EDAX analysis also shows sufficient amount of Cr and Ni to form protective spinels. Marginal percentage of Fe is also reported, showing probable formation of non protective oxide of Fe_2O_3.

Cross-Sectional Analysis of the Oxide Scales

Figure 6 (a) shows SEM micrograph of the uncoated T-91 boiler tube steel having a non protective oxide scale layer on the top surface. As evident from the EDAX analysis points 5, 6 and 7 shows high percentage of Fe and O, indicating the probability of formation of non-protective oxide of Fe_2O_3. The formation of non protective oxide is also validated by XRD analysis. Further in the subscale region shown by point 1, 2 and 3 indicate presence of Cr in minor percentage. Presence of Nb and Mo can also be seen in the EDAX analysis.

The EDAX analysis of 65%Cr_3C_2-35% (Ni-20Cr) coating shown in Fig. 6(b) shows rich percentage of Cr along with significant amount of Ni and O at the outer most point indicating formation of protective oxides and spinels of Ni and Cr as revealed by XRD analysis. Presence of significant amount of Cr and Ni along with O are suitable for generating protective oxides for combating corrosion attack of aggressive environment. EDAX analysis of the substrate shows high percentage of Fe along with other constituent elements. The weight percentage of Fe can be seen steeply declining after point 2 and weight percentage of Cr and Ni increasing steeply. Evidently presence of V in sufficient amount can also be noticed. Moreover presence of Nb at the outer layer has shown the diffusion of the elements from the substrate towards the coating.

Figure 6 (b) shows the EDAX analysis of 75% Cr_3C_2-25% (Ni-20Cr) coated sample. A thin oxide layer consisting of significant amount of Cr and O along with low percentage of Ni and Fe at point 8 indicating probability of formation of protective and non protective oxides. Weight percentage of Cr and Ni increases after point 2 in the coating region and variation in their percentage from point 3 onwards till point 7 shows the blending of Cr and Ni in the coating powder.

DISCUSSION

HVOF sprayed Cr_3C_2–NiCr coatings on T-91 boiler tube steel exhibits a dense, adherent and uniform splat like microstructure with porosity less than 2%. The deposition of coating in layers parallel to the substrate provides a necessary protection against corrosive species penetrating into the coating. The measured value of porosity is in good agreement with the findings of Hazoor Singh *et al.*, J.K.N. Murthy *et al.*, T. S. Sidhu *et al.*, Michael *et al.*, L. Fedrizzi *et al.*, and Buta Singh *et al.,* [20, 28–33].

The softer coatings are at more risk when subjected to erosion–corrosion attacks at elevated temperatures [34]. High microhardness value is believed to be due to the high kinetic energy acquired by the powder particle, which ensures a good cohesion, denser and more homogeneous structure, deformation reinforcement and oxides free spray process, as suggested by Mingxi *et al.*, Verdon *et al.*, and Hawthorne *et al.,* [35–37].

From the obtained results it can be interpreted that the value of microhardness increases with increase in the carbide phase present in the coating powder. The maximum value of 862 Hv hardness has been achieved for the coating having maximum amount of carbide phase i.e. 75% Cr_3C_2-25% (Ni-20Cr) coating. Some variation in microhardness of the coating as observed along the cross section may be because of microstructural changes across the cross section of the coatings and presence of porosity, oxides, inclusions, unmelted, melted, and partially melted powder particles as suggested by Staia *et al.*, [38]. The microhardness of HVOF coatings under study are in good agreement with the findings of Murthy *et al.*, Mathews *et al.*, Bin Yin *et al.*, Zorawski *et al.*, and Sidhu *et al.*, [29, 39–42].

HVOF sprayed coatings have proved to be very effective in the simulated environment and have shown much less degradation even after 50 cycles of corrosion exposure in Na_2SO_4-V_2O_5 molten salt environment under cyclic conditions and followed parabolic rate law of oxidation throughout the cyclic study. Slight deviation from parabolic rate law by the uncoated steel may be attributed to rapid growth of inhomogeneous oxides as opined by Bala *et al.*, Sidhu *et al.*, Kamal *et al.*, Singh *et al.*, and Choi *et al.*, [2, 20, 43–45].

The higher corrosion rate during initial hours of study might be attributed to the direct application of salt layer on the metallic surface which allow rapid oxygen pick up by a diffusion of oxygen through molten salt layer, resulting in earlier corrosive attack and the diffusion of corrosive species in the substrate [20]. Higher initial period weight gain results are in good agreement with the earlier studies by Bala (2010), Bhatia *et al*., (2014), Sidhu *et al.,* (2003), Tiwari and Prakash (1997) and Hamid *et al.,* (2003) for Hot corrosion studies of boiler tube steels in identical molten salt environment [2, 25, 33, 46–47]. After initial hours the rate of corrosion tends to become almost uniform in accordance to the results obtained by Sidhu *et al*., [20].

The intensive spalling of the scale in case of uncoated sample may be attributed to severe strain developed by the precipitation of Fe_2O_3 from the liquid phase as has also been reported by Sachs [47]. Whereas the scales formed on the coated specimens found to be intact and adherent throughout the study. Also presence of Mo in a thin layer might have imposed severe strain on the scale, because Mo oxides causes an alloy induced acidic flux which might have resulted in spallation, cracking and exfoliation of the oxide scale, these cracks might have allowed the corrosive molten salt contents to reach the metal substrate [48–49].

Formation of iron oxide as the main phase in the oxide scale of uncoated steel is in good agreement with the XRD results reported by Tiwari and Prakash, Das *et al*., and Kaur *et al*., during hot corrosion studies of boiler tubes steels in the similar environment [50–52]. The weak peaks of Cr_2O_3 along with major peaks of Fe_2O_3 as identified in the present study is obvious as the steel contains minor amount of Cr and similar results have also been reported by Bhatia *et al*., [24]. Further XRD results have been supported by the EDAX analysis, where similar type of elemental distribution was identified.

The higher parabolic rate constant for uncoated steel is a direct indicative of higher corrosion rate for these uncoated steels in comparison to the coated samples. The corrosion weight gain for 65% Cr_3C_2-35% (Ni-20Cr) coating was observed to be almost 10 times lower than the weight gain by uncoated steel as shown in Table 4. This coating has indicated minimum corrosion rate among all the coated steels. The sequence of corrosion resistance of coatings for T-91 boiler tube steel at 550°C followed the sequence:

65%Cr_3C_2-35% (Ni-20Cr) > 75%Cr_3C_2-25% (Ni-20Cr)

The corrosion resistance pattern followed by the coatings, clearly indicate that the coatings with higher percentage of NiCr binder has shown higher corrosion resistance. The 65%Cr_3C_2-35% (Ni-20Cr) coating has given the best protection to the substrate steel, which may be due to the formation of Cr_2O_3 and nickel-chromium spinel i.e. $NiCr_2O4$ as confirmed by XRD analysis. These phases are reported to be protective by Hamid *et al.,* and Sundararajan [53–54]. Similar finding has been reported by Sidhu *et al.,* in their studies of hot corrosion on NiCr and Cr_3C_2-NiCr coatings [20].

The presence of Cr_2O_3 as revealed by EDAX analysis for coated samples (Fig. 6 b-c) is the direct indicative of the presence of oxygen and chromium along the splat boundaries This chromium oxide (Cr_2O_3) phase is thermodynamically stable due to its high melting points as well as it forms a dense, continuous and adherent layers that grow relatively slow as suggested by Kamal *et al*., and Stott [43, 55]. The continuous band of Cr_2O_3 in the subscale and Cr_2O_3 along the splat boundaries will not allow any further transport of the oxidising species and the metallic ions as suggested by Nicholl *et al*., and Kamal *et al*., [56-57].

CONCLUSION

- Both the coatings have provided the requisite protection to the base steel in Na_2SO_4–60%V_2O_5 molten salt environment at 550°C by formation of protective oxides, like Cr_2O_3 and $NiCr_2O_4$.
- The 65%Cr_3C_2-35% (Ni-20Cr) composition of alloy powder deposited on boiler tube steel has provided best corrosion resistance followed by 75%Cr_3C_2-25% (Ni-20Cr) under study.
- Some elements of the substrate steel such as Fe and Mo showed a tendency of outward diffusion from the substrate towards the coating surface, whereas Cr, Ni along with V, S and O showed inward diffusion tendency.

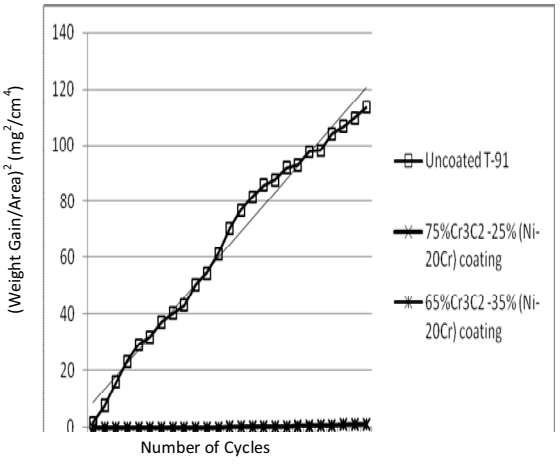

Fig. 2: Weight Gain Plot for Uncoated and Coated T-91 Boiler Tube Steel Samples Subjected to Corrosion in Molten Salt (Na_2SO_4-60%V_2O_5) Environment at 550°C for 50 Cycles

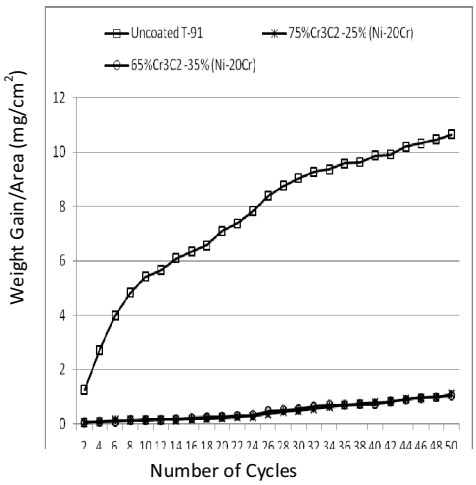

Fig. 3: (Weight Gain/ Area) 2 *vs.* Number of Cycles Plot for Coated and Uncoated Steels Subjected to Cyclic Oxidation for 50 Cycles in Na_2SO_4–60% V_2O_5

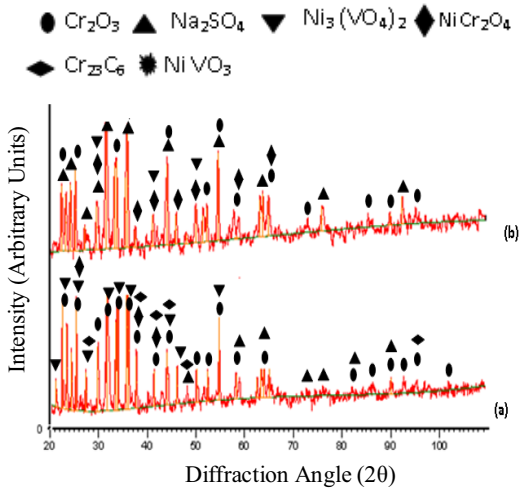

Fig. 4: X-ray Diffraction Profiles of Samples Subjected to Corrosion in Molten Salt (Na_2SO_4-60%V_2O_5) Environment at 550°C for 50 Cycles (a) 65%Cr_3C_2-35% (Ni-20Cr) Coating (b) 75%Cr_3C_2-25% (Ni-20Cr) Coating

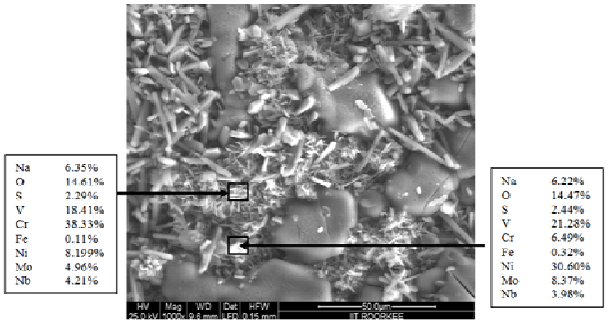

Fig. 5: SEM/EDAX Micrographs with EDS Spectrum of the 65%Cr3C2-35% (Ni-20Cr) Coating Showing Surface Morphology after Cyclic Corrosion in Na_2SO_4–60%V_2O_5 Environment for 50 Cycles at 550°C

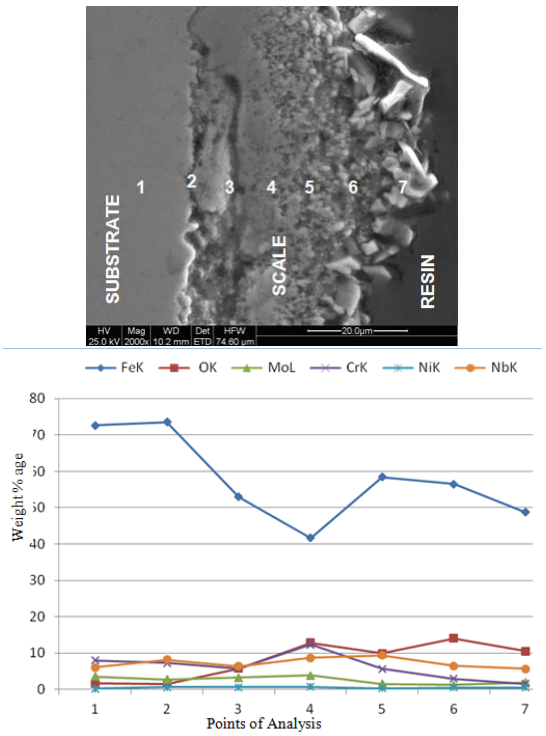

Fig. 6: (a) Cross-Sectional Analysis and Elemental Composition Variation of Uncoated T-91 Boiler Tube Steel Samples after Cyclic Hot Corrosion at 550°C in Na_2SO_4–60%V_2O_5 Environment for 50 Cycles

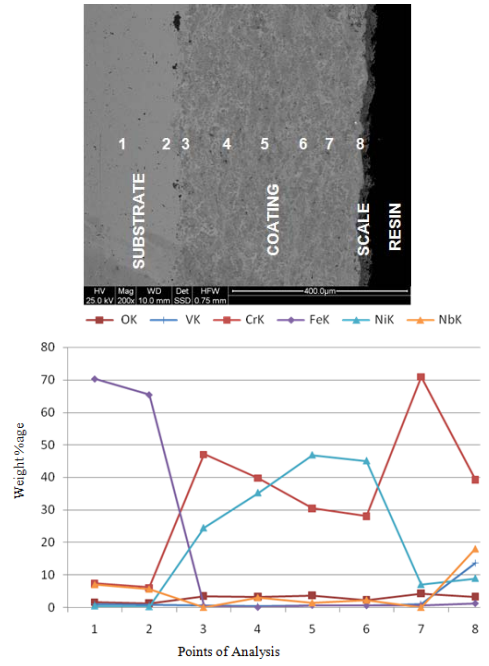

Fig. 6: (b) Cross-Sectional Analysis and Elemental Composition Variation of 65% Cr_3C_2-35% (Ni-20Cr) Coated T-91 Boiler Tube Steel Sample after Cyclic Hot Corrosion in Na_2SO_4–60%V_2O_5 Environment for 50 Cycles at 550°C

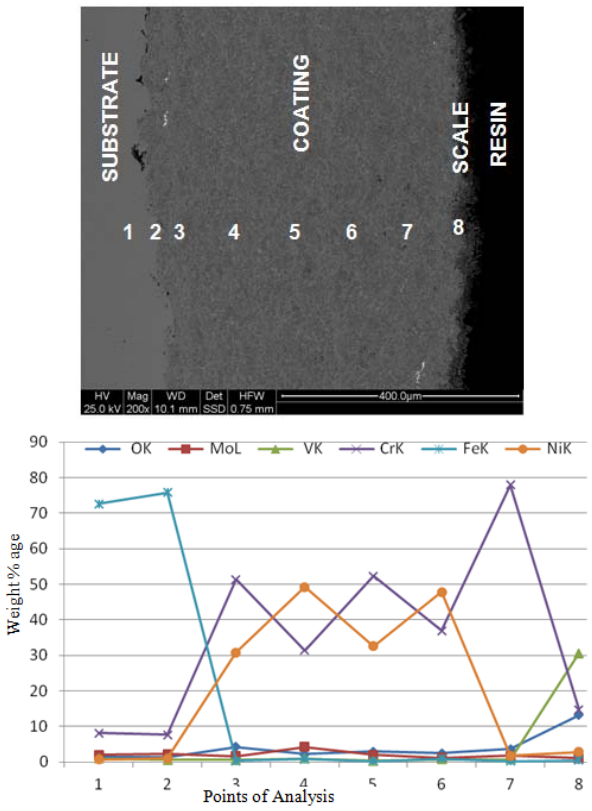

Fig. 6: (c) Cross-Sectional Analysis and Elemental Composition Variation of 75% Cr_3C_2-25% (Ni-20Cr) Coated T-91 Boiler Tube Steel Samples after Cyclic Hot Corrosion in Na_2SO_4–60% V_2O_5 Environment for 50 cycles at 550°C

REFERENCES

[1] Sidhu, B.S.; Puri, D.; and Prakash, S. (2004). Characterisations of Plasma Sprayed and Laser Remelted NiCrAlY Bond Coats and Ni_3Al Coatings on Boiler Tube Steels. Mater. Sci. Eng. A-Struct., 368 (1-2), 149-158.

[2] Bala, N.; (2010). Investigations on the Hot Corrosion Behaviour of Cold Spray and HVOF Spray Coatings on T22 and SA 516 Steels. Ph.D. Thesis, Mechanical Engineering Department, Punjab Technical University, Jalandhar, India.

[3] Kaushal, G.; Singh, H.; and Prakash, S.; (2011). High Temperature Erosion-Corrosion Performance of HVOF Sprayed Ni-20 Cr Coating in Actual Boiler Environment," Metallurgical and Materials Transactions-A. 42, 1836-1846.

[4] Natesan, K.; (1976). Corrosion-Erosion Behavior of Materials in a Coal-Gasification Environment. Corros., 32 (9), 364-370.

[5] Otero, E.; Merino, M.C.; Pardo, A.; Biezma, M.V.; and Buitrago, G. (1987), Study on Corrosion Products of IN657 Alloy in Molten Salts. Proc. of 10th ICMC, Madras, India. 4, 3583-3591.

[6] Kolta, G. A.; Hewaidy, L. F.; and Felix, N. S. (1972). Reactions between Sodium Sulphate and Vanadium Pentoxide. Thermo. Acta, 4, 151-164.

[7] Tiwari, S. N.; and Prakash, S., (1997). Studies on the Hot Corrosion Behaviour of Some Superalloys in Na_2SO_4-V_2O_5. Proc. of SOLCEC, Kalpakkam, India, C33.

[8] Hidalgo, V.H.; Varela, F.J.B.; Menendez, A.C.; and Martinez, S.P. (2001). A Comparative Study of High-temperature Erosion Wear of Plasma-sprayed NiCrBSiFe and WC-NiCrBSiFe Coatings under Simulated Coal-fired Boiler Conditions. Tribology, 34, 161-169.

[9] Eliaz, N.; Shemesh, G.; and Latanision, R.M. (2002). Hot Corrosion in Gas Turbine Components. Eng. Fail. Anal., 9, 31-43.

[10] Koch, G. H.; Brongers, M. P. H.; Thompson, N. G.; Virmani, Y. P.; and Payer, J. H. (2002). Historic Congressional Study: Corrosion Costs and Preventive Strategies in the United States. Supplement to Mater. Perfor., 1-11.

[11] Burakowski, T.; and Wierzchon, T. (1999). Surface Engineering of Metals, Principles, Equipment, Technology. CRC Press, N. W., Boca Raton, Florida.

[12] Matthews, A.; Artley, R. J.; and Holiday, P. (1998). Future's bright for surface engineering. Mater. World, 6, 346–347.

[13] Heath, G. R.; Heimgartner, P.; Irons, G.; Miller, R.; and Gustafsson, S. (1997). An Assessment of Thermal Spray Coating Technologies for High Temperature Corrosion Protection. Mater. Sci. Forum, 251-54, 809-816.

[14] Liu, Y.; Fischer, T. E.; and Dent, A. (2003). Comparison of HVOF and plasma-sprayed aluminaytitania coatings—microstructure, mechanical properties and abrasion behavior. Surf. Coat. Technol., 167, 68–76.

[15] Sidhu, H. S.; Sidhu B S.; and Prakash, S. (2010). Wear Characteristics of Cr_3C_2-NiCr and WC-Co Coatings Deposited by LPG Fueled HVOF. Tribol. Int., 43, 887-890.

[16] Khor, K.A.; and Leh, N. L. (1993). Proc. NTSC. 613.

[17] Kinos, T. (1994). Proc. NTPC, 357.

[18] Matthews, S.; Hyland, M.; and James, B. (2004). Long-Term Carbide Development in High-Velocity Oxygen Fuel/High-Velocity Air Fuel Cr_3C_2-NiCr Coatings Heat Treated at 900°C. J. Thermal Spray Technol., 13, (4), 526-536.

[19] Guilemany, J.M.; Espallargas, N.; Suegama, P.H.; and Benedetti, A.V. (2006). Comparative Study of Cr_3C_2-NiCr Coatings Obtained by HVOF and Hard Chromium Coatings. Corr. Sci., 48, 2998-3013.

[20] Sidhu, H.S.; Singh, B.S.; and Prakash, S. (2006). The Role of HVOF Coatings in Improving Hot Corrosion Resistance of ASTM-SA210 GrA1 Steel in the Presence of Na_2SO_4–V_2O_5 Salt Deposits. Surf. Coat. Technol., 200 (18-19), 5386-5394.

[21] Kaur, M. (2011). Studies on the Role of High Velocity oxy–Fuel Spray Coatings to Enhance Erosion-Corrosion resistance of Boiler Steels. Ph.D. Thesis. Mechanical Engineering Department, Punjab Technical University, Jalandhar, India.

[22] Tillmann, W,; Vogli, E.; Baumann, I.; Kopp, G.; Weihs, C. (2010). Desirability-Based Multi-Criteria Optimization of HVOF Spray Experiments to Manufacture Fine Structured Wear-Resistant 75Cr_3C_2-25(NiCr20) Coatings. J. Therm. Spray Technol. 19(1-2), 392–408.

[23] Matthews, S J.; James, B J.; and Hyland, M M. (2007), Microstructural influence on erosion behaviour of thermal spray coatings. Materials Characterization, 58, 59–64.

[24] Bhatia, R.; Singh, H.; and Sidhu, B. S. (2012). Characteristic Parameters and Erosion Behaviour of 65% Cr_3C_2–35% NiCr Coating. International Journal of Surface Engineering & Materials Technology, 3 (1), 2012.

[25] Stein, K.J.; Schorr, B.S.; and Marder, A.R.; (1999). Erosion of Thermal Spray MCr-Cr_3C_2 Cermet Coating. Wear, 224, 153-159.

[26] Bhatia, R.; Singh, H.; and Sidhu, B. S. (2014). Hot Corrosion Studies of HVOF-Sprayed Coating on T-91 Boiler Tube Steel at Different Operating Temperatures. Journal of Materials Engineering and Performance, 23(2),493-505.

[27] Sidhu, H.S.; Singh, B.S.; and Prakash, S. (2006) Mechanical and Microstructural Properties of HVOF Sprayed WC–Co and Cr_3C_2–NiCr Coatings on the Boiler Tube Steels using LPG as the Fuel Gas. J. of Mater. Process. Technol., 171, 77–82.

[28] Guilemany, J.M.; Fernandez, J.; Delgado, J.; Benedetti, A. V.; and Climent, F. (2002). Effects of Thickness Coatings on the Electrochemical Behavior of Thermal Spray Cr_3C_2-NiCr Coatings. Surf. Coat. Technol., 153, (2-3), 107-113.

[29] Murthy, J.K.N.; and Venkataraman, B. (2006). Abrasive wear behaviour of WC–CoCr and Cr_3C_2–20(NiCr) deposited by HVOF and detonation spray processes. Surf. Coat. Technol., 200, 2642–2652.

[30] Sidhu, T.S.; Prakash, S.; and Agrawal, R.D. (2006). Characterisation of NiCr Wire Coatings on Ni-and Fe-Based Superalloys by the HVOF Process. Surf. Coat. Technol., 200, (18-19), 5542-5549.

[31] Factor, M.; and Roman, I. (2002). Microhardness as a simple means of estimating relative wear resistance of carbide thermal spray coatings: Part 1. Characterization of Cemented Carbide Coatings. Journal of Thermal Spray Technology, 11 (4), 468-481.

[32] Fedrizzi, L.; Valentinelli, L.; Rossi, S.; and Segna, S. (2007). TriboCorrosion behavior of HVOF Cermet coatings. Corrosion Science, 49,2781-2799.

[33] Sidhu, B.S.; and Prakash, S. (2003). Evaluation of the Corrosion Behaviour of Plasma-Sprayed Ni_3Al Coatings on Steel in Oxidation and Molten Salt Environments at 900°C. Surf. Coat. Technol., 166, 89-100.

[34] Sidhu, B.S.; and Prakash, S. (2006). Erosion-Corrosion of Plasma as Sprayed and Laser Remelted Stallite-6 Coatings in a Coal Fired Boiler. Wear, 260, 1035-1044.

[35] Mingxi, L.; Yizhu, H.; and Guoxiong, S. (2004). Microstructure and wear resistance of laser clad cobalt-based alloy multi-layer coatings. Appl. surf. Sci., 230 (1-4),201-206.

[36] Verdon, C.; Karimi, A.; and Martin, J.L. (1998). A study of high velocity oxy-fuel thermally sprayed tungsten carbide based coatings. Part 1: Microstructures. Mater. Sci. Eng. A, 246, 11–24.

[37] Hawthorne, H.M.; Arsenault, B.; Immarigeon, J.P.; Legoux, J.G.; and Parameswaran, V.R. (1999), Comparison of slurry and dry erosion behaviour of some HVOF thermal sprayed coatings. Wear, 225–229, 825–834.

[38] Staia, M. H.; Valente, T.; Bartuli, C.; Lewis, D.B.; and Constable, C.P. (2001). Part I: Characterization of Cr_3C_2-25% NiCr Reactive Plasma Sprayed Coatings Produced at Different Pressures. Surf. Coat. Technol., 146-147, 553-562.

[39] Matthews, S.; Hyland, M.; and James, B. (2004). Long-Term Carbide Development in High-Velocity Oxygen Fuel/High-Velocity Air Fuel Cr_3C_2-NiCr Coatings Heat Treated at 900°C. J. Thermal Spray Technol., 13 (4), 526-536.

[40] Yin, B.; Liu, G.; Zhou, H; Chen, J.; and Yan, F. (2010). Sliding wear behavior of HVOF sprayed Cr3C2-NiCr/CeO2 Composite coatings at elevated temperature upto 800^0C. Tribology Letter, 37, 463-475.

[41] Wojciech, Ż. K. (2008). Scuffing resistance of plasma and HVOF sprayed WC12Co and Cr3C2-25(Ni20Cr) coatings. Surface and Coatings Technology, 202, 4453-4457.

[42] Sidhu, H. S.; Sidhu, B S.; and Prakash, S. (2010). Wear Characteristics of Cr_3C_2-NiCr and WC-Co Coatings Deposited by LPG Fueled HVOF. Tribol. Int., 43, 887-890.

[43] Kamal, S.; Jayaganthan, R.; Prakash, S.; and Kumar, S. (2008). Hot Corrosion Behavior of Detonation Gun Sprayed Cr_3C_2-NiCr Coatings on Ni and Fe-based Superalloys in Na_2SO_4-60%V_2O_5 Environment at 900°C. J. Alloys and Compounds, 463, (1-2), 358-372.

[44] Singh, H.; Puri, D.; Prakash, S.; and Maiti R, (2007). Characterization of oxide scales to evaluate high temperature oxidation behavior of Ni–20Cr coated superalloys. Materials Science and Engineering A, 464, 110–116.

[45] Choi, H.; Yoon, B.; Kim, H.; and Lee, C. (2002). Surf. Coat. Technol. 150 (2–3) 297–308.

[46] Tiwari, S. N.; and Prakash, S. (1997). Studies on the Hot Corrosion Behaviour of Some Superalloys in Na2SO4-V2O5. Proc. of SOLCEC, Kalpakkam, India, C33.

[47] Sachs, K. (1958). Accelerated High Temperature Oxidation Due to Vanadium Pentoxide. Metallurgia, 167-173.

[48] Sidhu, T.S.; Prakash, S.; and Agrawal, R.D. (2006). Hot Corrosion Studies of HVOF Sprayed Cr_3C_2-NiCr and Ni-20Cr coatings on a Nickel based Superalloy at 900ºC. Surf. Coat. Technol., 201, 792-800.

[49] Pettit, F. S.; and Meier, G. H. (1984). Oxidation and Hot corrosion of Superalloys. The Met. Soc. of AIME, Warrendale, Pensylvania, 651-687.

[50] Tiwari, S. N.; and Prakash, S. (1996). Hot Corrosion Behaviour of an Iron-Base Superalloy in Salt Environment at Elevated Temperatures. Proc. of Sympos. Metals and Materials Research, Indian Institute of Technology Madras, Madras, 107-117.

[51] Das, D.; Balasubramaniam, R.; and Mungole, M.N. (2002). Hot corrosion of Fe_3Al. J. Mater. Sci., 37 (6), 1135-1142.

[52] Kaur, M.; Singh, H.; and Prakash, S. (2009). High Temperature Corrosion Studies of HVOF Sprayed Cr_3C_2-NiCr Coating on SAE-347H Boiler Steel. J. Therm. Spray Technol., 18 (4), 619-632.

[53] Ul-Hamid, A. (2003). Diverse Scaling Behavior of the Ni-20Cr Alloy. Maters. Chem. Phys., 80, 135-142.

[54] Sundararajan, T.; Kuroda, S.; Itagaki, T.; and Abe, F. (2003). Steam Oxidation Resistance of Ni-Cr Thermal Spray Coatings on 9Cr-1Mo Steel. Part 1: 80Ni-20Cr. ISIJ Int., 43 (1), 95-103.

[55] Stott, F. H.(1998). The Role of Oxidation in the Wear of Alloys. Trib. Int., 31(1-3), 61-71.

[56] Nicoll, A.R.; and Wahl, G. (1983). The Effect of Alloying Additions on M-Cr-Al-Y Systems-An Experimental Study. Thin Solid Films, 95, 21-34.

[57] Kamal, S.; Jayaganthan, R.; Prakash, S. (2009). Evaluation of cyclic hot corrosion behaviour of detonation gun sprayed Cr 3 C 2–25 % NiCr coatings on nickel-and iron-based superalloys. Surface & Coatings Technology, 203(8), 1004-1013.